sustainability

MDPI

Article

Coagulation and Dissolution of CuO Nanoparticles in the Presence of Dissolved Organic Matter Under Different pH Values

Rizwan Khan [1], Muhammad Ali Inam [1], Saba Zam Zam [1], Muhammad Akram [2], Sookyo Shin [1] and Ick Tae Yeom [1,*]

[1] Graduate School of Water Resources, Sungkyunkwan University (SKKU), Suwon 16419, Korea; rizwankhan@skku.edu (R.K.); aliinam@skku.edu (M.A.I.); sabazamzam@skku.edu (S.Z.Z.); tkssk08@gmail.com (S.S.)

[2] Shandong Key Laboratory of Water Pollution Control and Resource Reuse, School of Environmental Science and Engineering, Shandong University, Qingdao 266200, China; m.akramsathio@mail.sdu.edu.cn

* Correspondence: yeom@skku.edu; Tel.: +82-312-996-699

Received: 26 April 2019; Accepted: 15 May 2019; Published: 17 May 2019

Abstract: The increased use of copper oxide nanoparticles (CuO NPs) in commercial products and industrial applications raises concerns about their adverse effects on aquatic life and human health. Therefore, the current study explored the removal of CuO NPs from water via coagulation by measuring solubility under various pH values and humic acid (HA) concentrations. The results showed that the media pH significantly affected the coagulation efficiency of CuO NPs (30 mg/L) under various (0–0.30 mM) ferric chloride (FC) dosages. The concentration of dissolved Cu^{2+} ions at pH 3–6 was (16.5–4.8 mg/L), which was higher than at other studied pH (7–11). Moreover, the simultaneous effect of coagulants and charge neutralization at pH 6–8 enhanced the removal of CuO NPs. At a lower FC (0–0.05 mM) dosage, the higher HA concentration inhibited the aggregation of CuO NPs. However, at the optimum dose of (0.2 mM) FC, the efficiency of turbidity removal and solubility of CuO NPs between pH 8 and 11 was above 98% and 5%, respectively, probably due to coagulant enmeshment. Our study suggested that coagulation was effective in removing the CuO NPs from the complex matrices with pH values ranging from 8–11. The findings of the present study provide insight into the coagulation and dissolution behavior of CuO NPs during the water treatment process.

Keywords: aggregation; coagulation; CuO; dissolution; humic acid; nanoparticles

1. Introduction

Many commercial products containing metal-based nanoparticles (NPs) are currently available in the market [1]. It is reported that every year around 28–32% of the discharged NPs are released into the surface waters of the United States. Thus, a large number of released NPs pose a potential risk to human health and aquatic life [2]. Copper oxides (CuO) are among the most widely used NPs in textiles, wood preservatives, electronics, inks, films, coatings, and ceramics, because of their specific structural properties [3,4]. The global annual production of CuO NPs was around 570 tons in 2014 and an estimated 1600 tons by 2025. Upon production and application, CuO NPs enter different environments such as natural surface waters and sediments, thereby increasing the risk of exposure to organisms as well as affecting their life cycle [2]. CuO NPs may dissociate into Cu^{2+} and higher concentrations significantly affect the growth of aquatic organisms, especially *lymphocytes*, *Fagopyrum esculentum*, and *Pseudokirchneriella* [5]. A recent study reported that the discharged NPs substantially inhibit the capability of wastewater biofilms [6]. The toxic effects of NPs on humans

via damage to DNA structure and cell membranes were also reported [7]. Thus, it is important to understand the dissolution phenomena of CuO NPs in the aquatic environment to minimize the related environmental and ecological risks of soluble engineered nanoparticles (ENPs) in general.

In the aquatic system, the dissolution of CuO NPs depends upon several factors such as particle size, shape, and surface charge, and physicochemical properties of the media, i.e., ionic strength (I.S), pH, and dissolved organic matter (DOM) [8]. A previous study reported that media pH strongly influenced the surface potential and dissolution of CuO NPs via protonation/deprotonation of surface hydroxyl groups [9]. For instance, a recent study showed that a decrease in the pH of aqueous environment enhanced the dissolution of ENPs [10]. Furthermore, natural waters also contain ubiquitous humic substances with concentrations of dissolved organic carbon ranging from 1–100 mg/L [11]. The DOM at a lower concentration (0.1 mg/L) might be adsorbed onto the NPs surface, resulting in a negative charge depending on various pH values to increase the stability of NPs suspension. Bian et al. reported that the polydentate structure of humic acid (HA) increases the dissolution of ZnO NPs at pH values ranging from 9–11 [12]. Furthermore, the rate of dissolution of NPs may be enhanced with increased HA concentration in the solution. Conversely, a recent study demonstrated that fulvic acid hindered the rate of carbon nanotubes dissolution and increased colloidal stability because of surface interaction [13]. A previous study showed that a coating of HA on the surface of CuO NPs resulted in particle disaggregation, and with further increase in HA concentration improved the dispersion of NPs [9]. Therefore, water contaminated with the CuO NPs enhances the risk of exposure to human and aquatic living organisms. Thus, it is important to consider the dissolution of CuO NPs in the treatment process, which is influenced by the solution chemistry.

Several advanced technologies, such as membrane filtration are used to remove NPs from water [14,15]. However, membrane fouling significantly affects performance and increases the cost of membrane treatment [15]. The particles can be removed via activated sludge, but most of the ENPs might be toxic to microorganisms as well as affect the overall sludge treatment by altering the sludge properties [16]. Coagulation is an efficient and simple process commonly used in water treatment to remove suspended solids, organic and inorganic substances from the water. Earlier studies [17–19] reported that NPs including cadmium telluride (CdTe), C(60), and multiwall carbon nanotubes (MWCNT) were efficiently removed from water by alum as well as polyaluminum chloride (PACl) coagulation. In addition, variable coagulation efficiencies of different ENPs, such as Ag (2–21%), ZnO (46–98%) and TiO_2 (2–9%) have also been reported [20]. The DOM has been found to hinder the agglomeration of TiO_2 NPs and affect the overall removal efficiency of the coagulation process [21]. For example, ZnO NPs coated with DOM such as HA and salicylic acid (SA) showed substantial adsorption capacities with increasing colloidal stability, thereby reducing the NPs removal because of electrostatic repulsion between organic molecules [22]. However, studies investigating the interactive behavior of CuO NPs in the presence of HA under different pH values were rarely investigated by environmental scholars. Furthermore, the studies also appear inadequate in elucidating the influence of HA on the dissolution and coagulation of CuO NPs. Thus, it is important to comprehensively understand the effect of HA on the removal of CuO NPs by coagulation in heterogenous water environments.

Accordingly, the present study investigated the effect of pH and HA on the removal of CuO NPs via coagulation from the water. In this study, we evaluated the removal efficiency by measuring the suspension turbidity and residual concentration of Cu^{2+} ions under different HA concentrations with varying pH values.

2. Materials and Methods

2.1. Chemicals Reagents and Stock Solution Preparation

The CuO NPs (CAS No: 1317380, purity ≥99.0%) with vendor reported diameter <50 nm were obtained from Sigma-Aldrich (St. Louis, MO, USA) and used without additional purification (Supplementary Materials [SM] Table S1). The CuO NPs stock suspension was prepared by weighing

3 mg of CuO powder and dispersion into 100 mL of 1 mM $NaHCO_3$ solution. The effect of the probe sonication on the turbidity of CuO NPs suspension was determined (Figure S1A). All suspensions were sonicated according to the optimized settings using an ultrasonicator (Bio-Safer 1200/90, Â 12 mm, Nanjing, China) for 30 min prior to coagulation experiments. The suspension pH was adjusted to 9 by 0.1 M HCl or 0.1 M NaOH solutions to reduce the effect of dissolution of CuO NPs during the sonication. Subsequently, 1 mL of the NPs suspension was transferred into a DTS0012 cuvette and placed in the Zetasizer sample chamber for hydrodynamic (HDD) size measurements, while the results were reported in intensity-volume % distribution. Humic acid (HA) with (99+% purity) was purchased from Sigma-Aldrich (St. Louis, MO, USA) and used as a model for dissolved organic matter (DOM). The stock solution of HA was prepared by dissolving 100 mg of HA powder in 100 mL of deionized (DI) water and adjusting the solution pH to 10 using 0.1 M NaOH in order to ensure complete dissolution of HA. The solution was stirred at 600 rpm for 24 h to increase the stability and then filtered with a 0.45 µm glass fiber filter followed by pH adjustment to 7. The total organic carbon (10 mg/L HA) was 4.5 mg/L. The coagulant iron (III) chloride hexahydrate ($FeCl_3{\cdot}6H_2O$) with (98+% purity) was purchased from local suppliers. Coagulant stock solution, i.e., 0.1 M FC was prepared by dissolving $FeCl_3{\cdot}6H_2O$ into DI water.

2.2. Coagulation and Dissolution

Coagulation experiments were performed in a jar tester (Model: SJ-10, Young Hana Tech Co., Ltd. Gyeongsangbuk-Do, Korea) as follows: Rapid mixing at 200 rpm within 1 min followed by slow mixing at 40 rpm for 15 min and settling for 30 min. The solubility of CuO NPs significantly increases at pH below 7 and above 11 as previously reported [23]. Systematic experiments were performed at pH values 3–11 to evaluate the effect of pH on the dissolution phenomena of CuO NPs. The performance was evaluated via measurement of supernatant turbidity after coagulation using a turbidimeter (Hach Benchtop 2100 N, Loveland, CO, USA). An aliquot of ~30 mL was then collected to measure the concentration of the dissolved Cu^{2+} and ferric (Fe^{3+}) ions via inductively coupled plasma optical emission spectrometry (ICP-OES: Model Varian, Agilent technologies, Sana Clara, CA, USA). In order to simulate the natural water conditions, the concentration of HA was maintained in the range of 0–10 mg/L (ref). The Visual MINTEQ 3.1 (KTH, Stockholm, Sweden) was used to determine the speciation of Cu and Fe(III) in aqueous media after coagulation with different HA concentrations. To further explore the impact of carbon dioxide (CO_2) on Cu and Fe(III) species, parallel tests were conducted with and without CO_2 in the system. Furthermore, all of the experiments were performed in triplicate, and the relative standard deviations (RSD) were reported.

2.3. Additional Characterization of CuO NPs

The specific surface area of CuO NPs was analyzed using the N_2-Brunauer Emmett Teller (BET) method (ASAP 2020, Micromeritics, Norcross, GA, USA). The zeta potential of CuO NPs was determined from their electrophoretic mobility using a Zetasizer analyzer (Malvern Nano-ZS, Worcestershire, UK) at 25 ± 1 °C. The particle size distribution of the CuO NPs in solution was measured using dynamic light scattering (DLS) with a He-Ne laser (λ = 632.8 nm).

3. Results and Discussion

3.1. Characteristics of CuO NPs

The CuO NPs were characterized in water immediately after sonication. As shown in Figure S1A, the optimal CuO NPs dispersion was obtained at a sonication time of 30 min; however, no significant difference in suspension turbidity was detected upon further increase in sonication time. Further, as shown in Figure S1B, the diameter of most particles was in the range of 150–250 nm suggesting a much larger size of CuO NPs in water compared with the reported primary particle size (<50 nm). The change in particle size may be due to an increase in van der Waals (vdW) forces among the NPs, resulting in the

formation of larger aggregates in solution [24]. The BET specific surface area of CuO NPs was found to be 29.2 m^2/g. The impact of pH on the dissolution and zeta potential of CuO (30 mg/L) suspension were investigated (Figure 1). It was obvious that the pH range of 2.0–6.9 facilitated the dissolution of CuO NPs, which was consistent with previous studies [9,23]. The Cu^{2+} released from CuO at pH range 2.0–5.0 was up to 19.8–8.4% of the total Cu. However, the solubility of CuO NPs declined above pH 7, and less than 1.3% of the total Cu was measured at pH 8. Under acidic environment, the interaction of H^+ ions with CuO NPs significantly released a large amount of Cu^{2+} ions, whereas at alkaline pH, the formation of $Cu(OH)^+$ complexes occurred due to the presence of high concentrations of OH^- ions [12]. Therefore, considering the dissolution of CuO NPs in highly acidic conditions, the coagulation experiments were conducted at pH 9 to minimize the NPs dissolution. Further, based on the speciation of Fe(III), large amounts of $Fe(OH)_2^+$ were generated around pH 8, which may facilitate the coagulation process (Figure S1C). The average zeta potential of CuO at pH 8 was +6.14 mV, which declined gradually with a pH increasing to more alkaline values. As shown in Figure 1, CuO NPs exhibit a stable and positive charge (+27.9 ± 1.3 mV) from pH 3.0–5.0. Subsequently, the zeta potential sharply decreased to the Isoelectric point (IEP) at a pHiep of approximately ~8.2 ± 0.1, which is consistent with earlier studies [9,23,25] investigating CuO NPs. Further increase in pH resulted in charge reversal with zeta potential values of −24.76 ± 1.3 mV at pH 11 ± 0.1. These results were consistent with previous study findings [25], suggesting that the surface potential was positive when pH < pHiep and negative at pH > pHiep. In addition, NPs with zeta potential below ±15 mV were supposed to be unstable, while NPs with zeta potential higher than ±30 mV were considered stable in the solution.

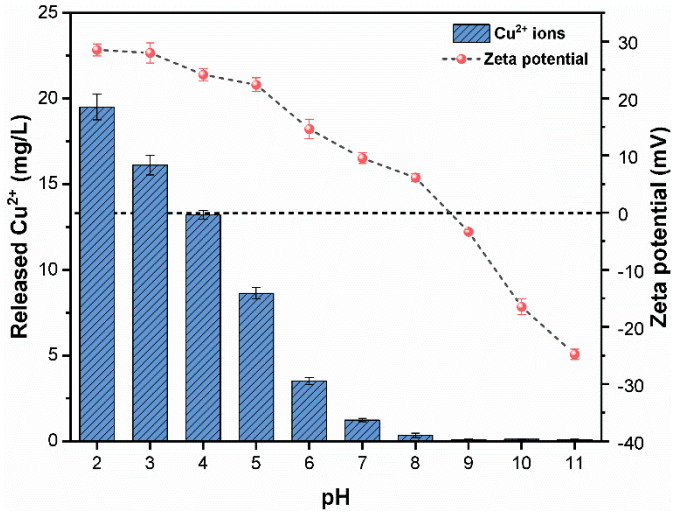

Figure 1. Cu^{2+} released (mg/L); and zeta potential of CuO NPs as a function of pH.

3.2. Effect of Coagulant Dose on CuO NPs Removal

Figure 2 illustrates the turbidity removal efficiency of CuO NPs (30 mg/L) at various FC dosages at pH 9. It can be seen that at a lower FC dosage (0–0.05 mM), the removal efficiency was below 60%, which may be attributed to fewer active Fe sites available in the solution. In addition, the inadequate compression of the electrical double layer (EDL) of NPs induced weak interparticle bridging among the colloidal flocs [18]. The turbidity removal efficiency was remarkably enhanced with increasing FC dose and the highest removal up to ~98% was obtained with 0.2 mM FC dosage. However, a further increase of coagulant dose (up to 0.30 mM) slightly decreased the turbidity removal efficiency of CuO NPs probably due to the charge inversion and restabilization of NPs flocs following oversaturation of polyelectrolytes [26]. In addition, as Figure 2 further suggests the addition of FC hinders the dissolution of CuO NPs at pH 9 and the FC dosage had a slight impact on the solubility of CuO NPs. The measured solubility of CuO NPs at optimum FC dosage (0.2 mM) was around 2%, which can be

ignored compared with the higher removal of NPs. In general, the coagulation was found to be an efficient process in removing the CuO NPs from aqueous solution at pH 9.

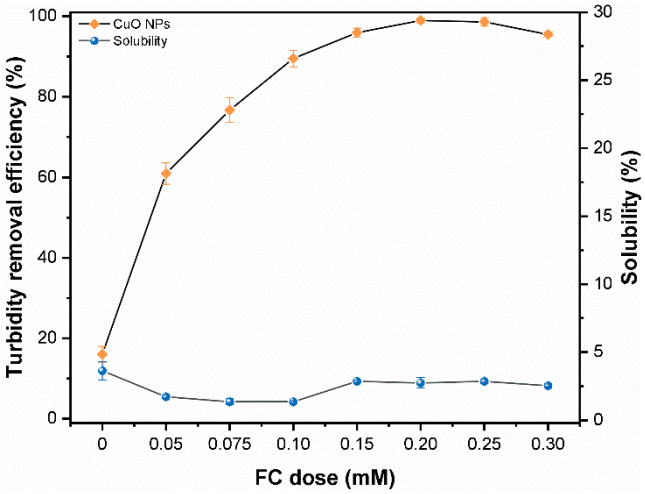

Figure 2. Effect of various FC (0–0.30 mM) dose on turbidity removal efficiency and solubility of CuO NPs (30 mg/L) at pH 9.

3.3. Effect of HA Concentration on CuO NPs Removal

The influence of HA concentration (10 mg/L) on the turbidity removal efficiency of CuO NPs (30 mg/L) was initially investigated at 0.05 mM FC dosage as a function of pH (Figure 3). The results indicated that the addition of HA decreased the coagulation efficiency of CuO NPs. The zeta potential of CuO at various HA concentration is shown in (Figure S2A,B), which suggests that the steric hindrance among NPs is further enhanced at higher HA concentration. The HA impeded the aggregation of CuO NPs and stabilized the negatively charged CuO NPs in solution. Mohd Omar et al. reported that the sorption of HA resulted in the disaggregation of NPs because of the Van der Walls (vdW) interaction between particles and HA molecules [27]. Furthermore, DOM has been known to stabilize the NPs by altering the zeta potential of the suspension from positive to negative. In order to further elucidate the effect of various HA concentrations on coagulation efficiency, an optimum dose of 0.2 mM was used in the following batch experiments.

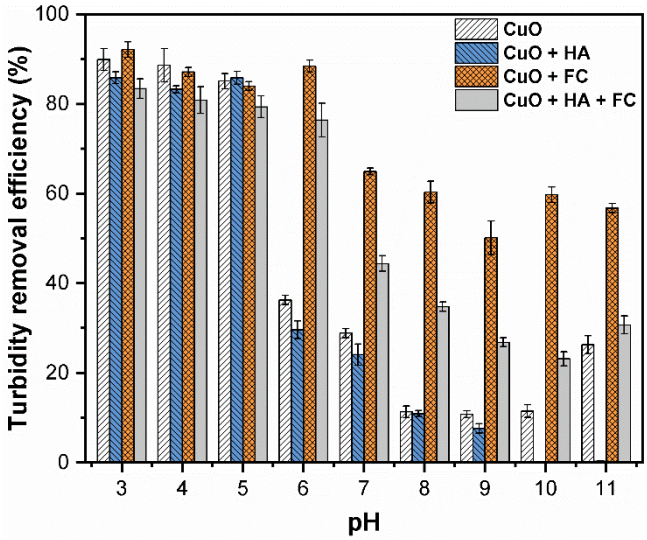

Figure 3. Turbidity removal efficiency of CuO NPs (30 mg/L) under different pH (3–11) values of FC (0.05 mM) and HA (10 mg/L).

It is noteworthy that in the absence of humic substance, the CuO NPs were dissolved under the highly acidic aqueous environment. Thus, CuO NPs were easily removed by coagulation at the pH range between 8 and 11 (Figure 4). In the absence of HA, the highest turbidity removal efficiency (99.1%) was obtained at pH 8 and 9, while the average removal efficiency was higher than 95%. At pH 8, the interaction between dominant Fe(III) species ($Fe(OH)_2^+$) and CuO NPs was increased via adsorption, resulting in higher turbidity removal [28]. Moreover, the coagulation efficiency increased with increased solution pH (9–10), which might be related to the enmeshed FC coagulants (Figure S1C). However, under highly alkaline pH (above 10), the effect of enmeshment was weaker due to the increased concentrations of $Fe(OH)_4^-$ species in the solution, which increased the electrostatic repulsion between negatively charged CuO NPs and $Fe(OH)_4^-$ (Figures S3A and S4A). Therefore, a slight decrease in the removal of CuO NPs above pH 10 was observed during the coagulation.

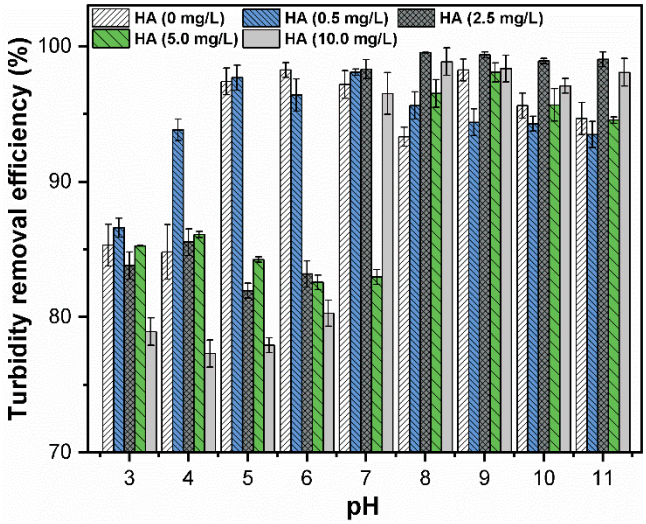

Figure 4. Efficiency of turbidity removal by CuO NPs (30 mg/L) under various pH (3–11) values and concentrations of HA (0, 0.5, 2.5, 5, 10 mg/L) at optimum FC (0.2 mM) dosage.

In addition, the CuO NPs were effectively removed even in the presence of HA when pH ranged between 8 and 11 (Figure 4). However, the higher concentration of HA significantly reduced the removal of CuO NPs at pH 3 and 6 compared with a lower concentration. The higher concentration of HA reverses the zeta potential from +6.14 to −45.2 mV (Figure S2A). However, the surface charge plays an insignificant role in the efficient removal of turbidity. The measured zeta potential of CuO NPs after coagulation experiment is shown in Figure S2B, which further explains the removal phenomena of CuO NPs from the heterogeneous environment. The possible removal mechanism might be related to the sufficient dosage of coagulant (0.2 mM FC), since the aqueous environment with pH greater than 8 was conducive to the formation of Fe(III) flocs (Figure S1C). Nonetheless, negatively charged CuO NPs, HA and $Fe(OH)_4^-$ (Figures S3A and S4A) were present in the solution. Therefore, the enmeshment of FC was stronger compared with the electrostatic repulsive forces among the NPs, which played a critical role in the removal of CuO NPs from aqueous solution. Moreover, the speciation of Cu and Fe(III) based on the presence of CO_2 after the completion of experiments to elucidate the role of CO_2 in the removal process (Figures S3 and S4). The results suggested that the presence of CO_2 at pH 6 and 11 enhanced the concentrations of $[Fe(OH)^2]^+$ and $[Fe(OH)_4]^-$, respectively. Moreover, ferric species preferably combine with the hydroxyl group. Based on these observations, it can be concluded that the combined effects of the enmeshment of coagulants and charge neutralization mechanism contributed to robust removal of CuO NPs from the water.

3.4. Effect of pH and HA on the Dissolution of CuO NPs

In the natural environment, the fluctuations in pH and the interaction between CuO NPs and humic substances affect the dissolution phenomena and increase their bioavailability in aquatic organisms. It has been proposed that after coagulation, the solution can be divided into three different segments including Cu^{2+}, suspended CuO NPs and CuO NPs flocs. Thus, the solubility of CuO NPs was determined via measurement of residual Cu^{2+} concentration in the solution (Figure 5). The results indicated that in the absence of HA, the solubility of CuO NPs was reduced with increasing solution pH and significantly decreased when the pH value was changed from 6–7. Figures S3A and S4A represent the dominant Cu species in the preferred pH range (3–11).

When pH ranged between 3–6, the concentration of Cu^{2+} ions in the supernatants was around 13 mg/L, which suggested that about 54.10% of NPs were dissolved in the aqueous solution because of the effect of protonation on the surface of CuO [12]. Hence, under highly acidic conditions, the turbidity removal of CuO NPs resulted from dissolution rather than coagulation. However, the measured concentration of Cu^{2+} at pH 9 was approximately 0.52 mg/L, while the total amount of copper species in the supernatant was 23.87 mg/L. The average solubility and turbidity removal at pH 9 and 11 were nearly 3.54% and 96.87%, respectively, which further indicated that coagulation is an effective method to remove CuO NPs from aqueous solution. These results are consistent with a previous study [29], which reported that at pH below 7, the dominant forms of copper were Cu^{2+} and $Cu(OH)^{+}$. However, at pH values above 9, the dissolution of CuO NPs occurred due to soluble hydroxy and hydroxide complexes. Therefore, the solubility of CuO NPs at pH 9 was less compared with highly acidic conditions. The possible chemical reactions of CuO NPs that may occur in highly acidic and alkaline conditions are as follows [30].

$$CuO\ (s) + 2H^{+}(aq) \leftrightarrows Cu^{+}(aq) + H_2O\ (l) \quad (1)$$

$$CuO(s) + H^{+}(aq) \leftrightarrows Cu(OH)^{+}(aq) \quad (2)$$

$$CuO(s) + OH^{-}(aq) + H_2O(l) \leftrightarrows CU(OH)_3^{-}(aq) \quad (3)$$

$$CuO(s) + 2OH^{-}(aq) + H_2O(I) \rightleftarrows Cu(OH)_4^{2-}(aq) \quad (4)$$

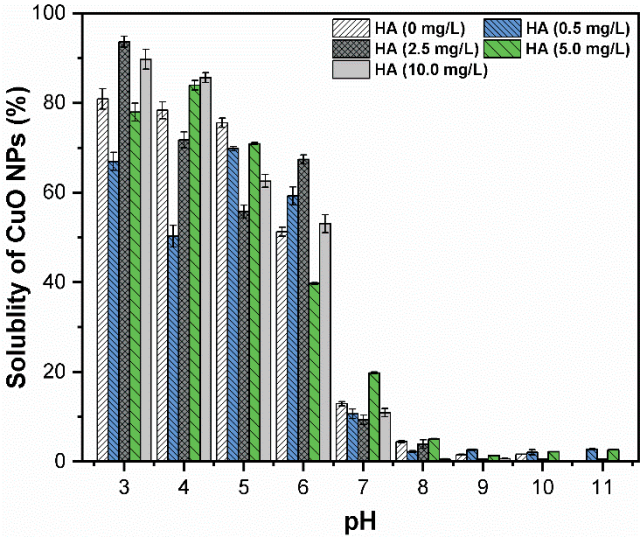

Figure 5. Solubility of CuO NPs (30 mg/L) under various pH (3–11) values and concentrations of HA (0, 0.5, 2.5, 5, and 10 mg/L) at FC (0.2 mM) dosage.

In addition, at a pH of 6–9, the presence of humic substances reduced the solubility with increasing pH, and the major speciation of copper ions is shown in Figures S3B and S4B. The lower concentration of HA inhibited the dissolution of CuO NPs suspension due to adsorption of organic molecules on the surface of NPs [13,22]. Moreover, the change in pH was also monitored before and after the coagulation experiment, which indicated a slight variation in pH, and an insignificant role in the dissolution of CuO NPs (Figure S5A,B). These findings have practical implications in that the presence of HA decreases the release of Cu^{2+} ions and reduces the associated risk and toxicity to aquatic life. Furthermore, HA has an insignificant effect on the coagulation efficiency of CuO NPs under alkaline conditions. In general, these results indicate that the coagulation process effectively removes the CuO NPs from the solution at a pH range of 8–11.

4. Conclusions

This study demonstrated that coagulation is an effective method to remove CuO NPs from the aqueous environment. However, the removal efficiency depends on the coagulant dosage used and the media pH. The results indicate that at a pH range of 8–11, the removal efficiency of CuO NPs (30 mg/L) at the optimum dose FC (0.2 mM) dose was higher than 98%, whereas the removal decreased under highly acidic pH conditions. Furthermore, when the pH ranged from 3–6, the dissolution of CuO NPs mainly occurred and was followed by the transformation of the released Cu into soluble hydroxide, hydroxy complex, and Cu^{2+} in the supernatant. However, at pH 6–8, the removal of CuO NPs resulted from the combined effects of charge neutralization as well as adsorption. In addition, the effect of the enmeshment of coagulants was stronger when the pH was between 8 and 11, which played a vital role in the removal of CuO NPs from the water. These results indicated that media pH and HA concentration influence the fate, mobility, and coagulation performance of ENPs in water/wastewater treatment.

Supplementary Materials: The following additional materials are available online at http://www.mdpi.com/2071-1050/11/10/2825/s1, **Figure S1**. (A) Effects of sonication time (5–40 min) on the turbidity of CuO NPs stock suspension (30 mg/L) at pH 9; (B) size distribution by volume (%) of CuO NPs at the optimized time (30 min) of sonication; (C) speciation of Fe (III) as a function of solution pH. **Figure S2**. Measured zeta potential of CuO NPs at different pH values (3–11) and HA concentrations (0.5, 2.5, 5, and 10 mg/L); (A) without FC; (B) with (0.2 mM) FC dosage. **Figure S3**. The species of Fe(III) and Cu ions in the supernatant after coagulation without CO_2 showing (A) HA = 0 mg/L; (B) HA = 10 mg/L. **Figure S4**. The species of Fe(III) and Cu ions in the supernatant after coagulation with CO_2 (A) HA = 0 mg/L; (B) HA = 10 mg/L. **Figure S5**. Change in pH before and after coagulation experiments of CuO NPs (30 mg/L) with 0.2 mM FC dosage (A) HA = 0 mg/L; (B) HA = 10 mg/L. **Table S1**: Physicochemical properties of CuO NPs used in the current study.

Author Contributions: R.K. and I.T.Y. designed the study; R.K. and M.A.I. performed the experiment and analyzed the data; and M.A. S.Z.Z, M.A. and S.S. provided critical feedback and directed the research program; R.K. wrote the final version of the manuscript.

Funding: The BK21 plus program supported this work through the National Research Foundation of Korea (NRF), funded by the Ministry of Education of Korea (Grant No. 22A20152613545).

Acknowledgments: The authors acknowledge the help of Adeela Hanif and Muhammad Haroon for their support in measurements and provision of critical feedback. The staff members of Zero Emission Center at Sungkyunkwan University are also acknowledged for their support in measurements and data reduction.

Conflicts of Interest: The authors declare the absence of any conflict of interest.

References

1. Vance, M.E.; Kuiken, T.; Vejerano, E.P.; McGinnis, S.P.; Hochella Jr, M.F.; Rejeski, D.; Hull, M.S. Nanotechnology in the real world: Redeveloping the nanomaterial consumer products inventory. *Beilstein J. Nanotechnol.* **2015**, *6*, 1769–1780. [CrossRef] [PubMed]
2. Keller, A.A.; Vosti, W.; Wang, H.; Lazareva, A. Release of engineered nanomaterials from personal care products throughout their life cycle. *J. Nanopart. Res.* **2014**, *16*, 2489. [CrossRef]
3. Gawande, M.B.; Goswami, A.; Felpin, F.-X.; Asefa, T.; Huang, X.; Silva, R.; Zou, X.; Zboril, R.; Varma, R.S. Cu and Cu-Based Nanoparticles: Synthesis and Applications in Catalysis. *Chem. Rev.* **2016**, *116*, 3722–3811. [CrossRef] [PubMed]

4. Ju-Nam, Y.; Lead, J.R. Manufactured nanoparticles: an overview of their chemistry, interactions and potential environmental implications. *Sci. Total Environ.* **2008**, *400*, 396–414. [CrossRef] [PubMed]
5. Aruoja, V.; Dubourguier, H.-C.C.; Kasemets, K.; Kahru, A. Toxicity of nanoparticles of CuO, ZnO and TiO_2 to microalgae Pseudokirchneriella subcapitata. *Sci. Total Environ.* **2009**, *407*, 1461–1468. [CrossRef] [PubMed]
6. Zheng, X.; Wu, R.; Chen, Y. Effects of ZnO nanoparticles on wastewater biological nitrogen and phosphorus removal. *Environ. Sci. Technol.* **2011**, *45*, 2826–2832. [CrossRef]
7. Dreher, K.L. Health and environmental impact of nanotechnology: toxicological assessment of manufactured nanoparticles. *Toxicol. Sci.* **2004**, *77*, 3–5. [CrossRef] [PubMed]
8. Son, J.; Vavra, J.; Forbes, V.E. Effects of water quality parameters on agglomeration and dissolution of copper oxide nanoparticles (CuO-NPs) using a central composite circumscribed design. *Sci. Total Environ.* **2015**, *521*, 183–190. [CrossRef]
9. Peng, C.; Shen, C.; Zheng, S.; Yang, W.; Hu, H.; Liu, J.; Shi, J. Transformation of CuO Nanoparticles in the Aquatic Environment: Influence of pH, Electrolytes and Natural Organic Matter. *Nanomaterials* **2017**, *7*, 326. [CrossRef]
10. Zhang, H.; Chen, B.; Banfield, J.F. Particle size and pH effects on nanoparticle dissolution. *J. Phys. Chem. C* **2010**, *114*, 14876–14884. [CrossRef]
11. Wall, N.A.; Choppin, G.R. Humic acids coagulation: influence of divalent cations. *Appl. Geochem.* **2003**, *18*, 1573–1582. [CrossRef]
12. Bian, S.W.; Mudunkotuwa, I.A.; Rupasinghe, T.; Grassian, V.H. Aggregation and dissolution of 4 nm ZnO nanoparticles in aqueous environments: Influence of pH, ionic strength, size, and adsorption of humic acid. *Langmuir* **2011**, *27*, 6059–6068. [CrossRef]
13. Yang, K.; Xing, B. Adsorption of fulvic acid by carbon nanotubes from water. *Environ. Pollut.* **2009**, *157*, 1095–1100. [CrossRef]
14. Zhong, Z.; Li, W.; Xing, W.; Xu, N. Crossflow filtration of nanosized catalysts suspension using ceramic membranes. *Sep. Purif. Technol.* **2011**, *76*, 223–230. [CrossRef]
15. Springer, F.; Laborie, S.; Guigui, C. Removal of SiO_2 nanoparticles from industry wastewaters and subsurface waters by ultrafiltration: Investigation of process efficiency, deposit properties and fouling mechanism. *Sep. Purif. Technol.* **2013**, *108*, 6–14. [CrossRef]
16. Tiede, K.; Boxall, A.B.A.; Wang, X.; Gore, D.; Tiede, D.; Baxter, M.; David, H.; Tear, S.P.; Lewis, J. Application of hydrodynamic chromatography-ICP-MS to investigate the fate of silver nanoparticles in activated sludge. *J. Anal. At. Spectrom.* **2010**, *25*, 1149–1154. [CrossRef]
17. Zhang, Y.; Chen, Y.; Westerhoff, P.; Crittenden, J.C. Stability and removal of water soluble CdTe quantum dots in water. *Environ. Sci. Technol.* **2007**, *42*, 321–325. [CrossRef]
18. Hyung, H.; Kim, J.-H.H. Dispersion of C60in natural water and removal by conventional drinking water treatment processes. *Water Res.* **2009**, *43*, 2463–2470. [CrossRef]
19. Holbrook, R.D.; Kline, C.N.; Filliben, J.J. Impact of source water quality on multiwall carbon nanotube coagulation. *Environ. Sci. Technol.* **2010**, *44*, 1386–1391. [CrossRef]
20. Abbott Chalew, T.E.; Ajmani, G.S.; Huang, H.; Schwab, K.J. Evaluating nanoparticle breakthrough during drinking water treatment. *Environ. Health Perspect.* **2013**, *121*, 1161–1166. [CrossRef]
21. Wang, H.T.; Ye, Y.Y.; Qi, J.; Li, F.T.; Tang, Y.L. Removal of titanium dioxide nanoparticles by coagulation: effects of coagulants, typical ions, alkalinity and natural organic matters. *Water Sci. Technol.* **2013**, *68*, 1137–1143. [CrossRef] [PubMed]
22. Khan, R.; Inam, M.; Park, D.; Zam Zam, S.; Shin, S.; Khan, S.; Akram, M.; Yeom, I. Influence of Organic Ligands on the Colloidal Stability and Removal of ZnO Nanoparticles from Synthetic Waters by Coagulation. *Processes* **2018**, *6*, 170. [CrossRef]
23. Khan, R.; Inam, M.A.; Park, D.R.; Khan, S.; Akram, M.; Yeom, I.T. The Removal of CuO Nanoparticles from Water by Conventional Treatment C/F/S: The Effect of pH and Natural Organic Matter. *Molecules* **2019**, *24*, 914. [CrossRef] [PubMed]
24. Keller, A.A.; Wang, H.; Zhou, D.; Lenihan, H.S.; Cherr, G.; Cardinale, B.J.; Miller, R.; Zhaoxia, J.I. Stability and aggregation of metal oxide nanoparticles in natural aqueous matrices. *Environ. Sci. Technol.* **2010**, *44*, 1962–1967. [CrossRef]

25. Miao, L.; Wang, C.; Hou, J.; Wang, P.; Ao, Y.; Li, Y.; Lv, B.; Yang, Y.; You, G.; Xu, Y. Effect of alginate on the aggregation kinetics of copper oxide nanoparticles (CuO NPs): bridging interaction and hetero-aggregation induced by Ca^{2+}. *Environ. Sci. Pollut. Res.* **2016**, *23*, 11611–11619. [CrossRef]
26. Zhang, L.; Mao, J.; Zhao, Q.; He, S.; Ma, J. Effect of AlCl3 concentration on nanoparticle removal by coagulation. *J. Environ. Sci.* **2015**, *38*, 103–109. [CrossRef]
27. Omar, F.M.; Aziz, H.A.; Stoll, S. Aggregation and disaggregation of ZnO nanoparticles: influence of pH and adsorption of Suwannee River humic acid. *Sci. Total Environ.* **2014**, *468*, 195–201. [CrossRef] [PubMed]
28. Tang, H.X. Inorganic polymer flocculation theory and flocculants. *China Build. Ind. Press. Peking* **2006**.
29. Zirino, A.; Yamamoto, S. A pH-dependent model for the chemical speciation of copper, zinc, cadmium, and lead in seawater. *Limnol. Oceanogr.* **1972**, *17*, 661–671. [CrossRef]
30. Albrecht, T.W.J.; Addai-Mensah, J.; Fornasiero, D. Effect of pH, concentration and temperature on copper and zinc hydroxide formation/precipitation in solution. In Proceedings of the Chemeca 2011: Engineering a Better World, Sydney Hilton Hotel, NSW, Australia, 18–21 September 2011; pp. 2100–2110.

© 2019 by the authors. Licensee MDPI, Basel, Switzerland. This article is an open access article distributed under the terms and conditions of the Creative Commons Attribution (CC BY) license (http://creativecommons.org/licenses/by/4.0/).